15

Pyroelectric effect in doped nonpolar glycine crystals

© G.Yu. Sotnikova,[1] P.S. Zelenovskiy,[2] A.D. Ushakov,[2] G.A. Gavrilov,[1] V.Ya. Shur,[2] A.L. Kholkin[2]

[1] Ioffe Institute,
St. Petersburg, Russia
[2] Institute of Natural Sciences and Mathematics, Ural Federal University named after the first President of Russia B.N. Yeltsin, Yekaterinburg, Russia
e-mail: kholkin@urfu.ru

Received October 22, 2022
Revised February 27, 2023
Accepted February 28, 2023

Doping-induced local symmetry breaking of centrosymmetric molecular crystals endows them with piezoelectric and pyroelectric properties. In this work, we measured temperature dependences of pyroelectric and piezoelectric coefficients in α–glycine crystals single-doped by threonine and double-doped by threonine and alanine. We analyzed primary and secondary pyroelectric effects in these crystals and suggested a model of the dopant complexes related to the observed effects.

Keywords: pyroelectricity, α-glycine, doped molecular crystals.

DOI: 10.21883/TP.2023.05.56076.214-22

Introduction

The pyroelectric effect, which consists in changing the spontaneous polarization of a crystal with a uniform change in its temperature [1], is actively used in various devices for registering electromagnetic radiation in a wide range of frequencies and intensities, thermal radiation detectors, pyrometers, thermal imagers, and is also one of the basic principles of collecting electricity from heat in energy harvesting devices [2–6]. This effect is observed in many polar organic and inorganic crystals (mainly ferroelectrics), polymers and biomaterials [7].

The pyroelectric effect measured in experiments is a combination of two contributions. On the one hand, a change in the crystal temperature leads to a redistribution of dipole moments in the crystal cell and, consequently, the generation of electric charges on the surface. This is the primary pyroelectric effect. On the other hand, the crystal is deformed as a result of heating and charges are redistributed due to the piezoelectric effect. This is a secondary pyroelectric effect [8]. In some cases associated with inhomogeneous heating of the material, it is also possible to talk about the tertiary effect, but it is negligible compared to the primary and secondary effects [9]. Since the relative contribution of these effects is determined by the properties of the material, their separate analysis can provide important information about the nature of pyroelectricity. While the secondary pyroelectric coefficient can be calculated using the coefficients of thermal expansion, elastic deformation and piezoelectric coefficients [8], direct measurements of the primary effect are fraught with great experimental difficulties, and therefore such studies are quite rare [10–13].

Experimental separation of primary and secondary pyroelectric effects is especially important for mixed molecular crystals, in which the introduction of various dopants can induce piezoelectric and pyroelectric properties in different manner [14] For example, doping of triglycine sulfate (TGS) with other amino acids significantly changes its electrical, pyroelectric and electromechanical properties [15–17]. Thus, molecular doping can be a promising method of controlling the functional properties of molecular and bioorganic materials, while a detailed study of this process is an urgent topic of modern studies [14,18,19]. From a microscopic point of view, polarization in mixed crystals can occur either due to the intrinsic dipole moments of dopants, or due to asymmetric disturbances in the crystal lattice of the host material caused by the introduction of dopants [14]. These mechanisms operate simultaneously in mixed crystals, and estimating their relative contributions is a difficult task. However, these mechanisms are closely related to primary and secondary pyroelectric effects, so their separation can provide important information about the interaction between dopants and the host crystal.

In this paper, the nature of the pyroelectric effect in α-glycine crystals doped with threonine alone or co-doped with threonine and alanine is studied. For glycine crystals, alanine is the most effective dopant of the substitution type, since their molecules have a similar structure, but the alanine molecule is larger than the glycine molecule, therefore, when it is introduced into the crystal lattice, a local field of mechanical stresses arises [20]. The threonine molecule, in turn, is somewhat larger than the alanine molecule and contains an additional polar group, which makes it possible to study in more detail and separate the contributions of mechanical stresses and dipole moments introduced by dopants to the induced polarization of α-glycine crystals. In this paper, temperature dependences of pyroelectric and piezoelectric coefficients are measured, primary and secondary pyroelectric effects in these crystals

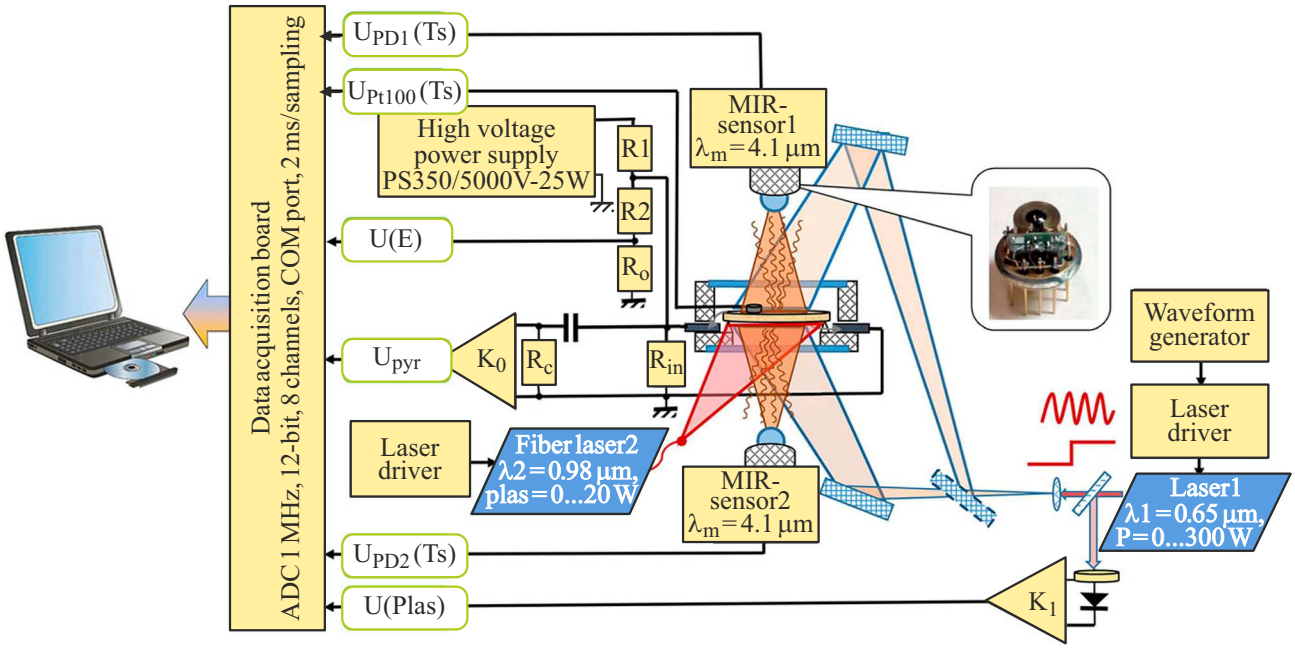

Figure 1. Schematic diagram of an experimental setup for pyroelectric measurements [22].

are analyzed, and a microscopic model of dopant complexes that cause the observed effects is proposed.

1. Materials and methods

Crystals of α-glycine (space group $P2_1/n$) doped with threonine molecules (Gly-Thr) were obtained by slow evaporation at a temperature of 23°C of an aqueous solution of glycine (Alfa Aesar, 99.5%) in the presence of 0.5 wt.% *L*-threonine (T-Fisher Scientific, 99.0%). Glycine crystals with double doping with alanine and threonine (Gly-Ala+Thr) were obtained using a similar method, but with an additional 0.5 wt.% *L*-alanine (Sigma Aldrich, $\geq$ 98%). No seeds were added to the solution. No preliminary processing of materials was carried out. The grown crystals had a well-faceted shape with a flat surface oriented perpendicular to the crystallographic axis (010) [21]. Raman spectra measured on the obtained crystals (data are not given) showed that such a small fraction of dopants does not affect the phase composition of the crystals formed.

Pyroelectric measurements were carried out by the Laser-Intensity Modulation Method (LIMM) [22]. The studied crystals were placed in a free state on a Teflon ring to prevent possible mechanical deformations, and they were illuminated simultaneously by two lasers (Fig. 1): *1* — visible laser radiation with a wavelength of 635 nm and adjustable power up to 120 mW was created by a semiconductor laser module STLL-MM-635-120-S3 (Stronglaser, Russia) and modulated using an external pulse generator with a frequency of 0.5 Hz to create a harmonic thermal effect required for pyroelectric measurements; *2* — infrared (IR) laser radiation with a wavelength of 960 nm and adjustable power up to 10 W was created by a high-power LATUS laser (ATC-Semiconductor Devices, Russia) and used to heat the sample to the required operating temperatures (up to 150°C). The temperature of the sample was determined contactless using an IR photodiode PD42S (IoffeLED Ltd, Russia) with a time resolution of 2 ms and an accuracy of 0.1°C. The area on which the measurement was performed was about 3 mm^2. The combination of non-contact sample heating and non-contact temperature determination allows carrying out pyroelectric measurements of both bulk samples and thin films with an accuracy significantly superior to traditional methods [22].

It should be noted that various types of temperature modulation were used to determine the magnitude and sign of the pyroelectric coefficient of the sample. This approach is based on the basic principles of the theory of information and measurement systems, where harmonic signals of different frequencies are used to determine the parameters of a dynamic system in the frequency domain, and a step function — for the analysis of its behavior in the time domain [22].

For recording pyroelectric current, I_{pyr}, metal electrodes with a thin layer of absorbing material increasing the absorption of heating IR laser radiation were applied to the upper and lower surfaces of the sample. The pyroelectric current was measured using a voltage amplifier with a conversion factor of $K_U = 100$ and an input resistance 10 MΩ. Thus, the conversion of current to voltage was performed using the conversion coefficient $K_I = 10^9$ V/A ($U_{pyr} = K_I I_{pyr}$). The measurement error was 0.3–3 pA. In harmonic laser exposure mode, the pyroelectric coeffi-

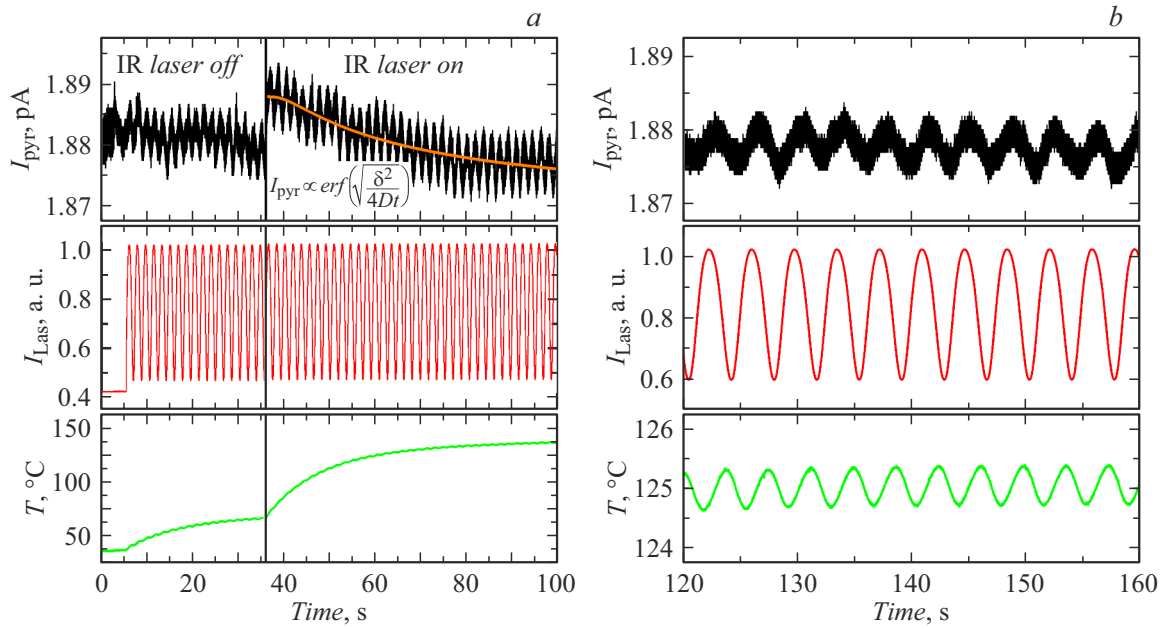

Figure 2. *a* — time dependencies of the pyroelectric current (black line), intensity of modulating laser radiation (red line (in online version)) and sample temperature (green line (in online version)) for the Gly-Thr crystal. The orange line (in online version) is an approximation of the relaxing part of the curve I_{pyr} after switching on the IR laser. The insert shows the function used for fitting the experimental data. *b* — time changes of pyroelectric current I_{pyr} in the equilibrium state, intensity of modulating laser radiation and sample temperature at operating temperature 125°C.

cient, p, was determined by the formula

$$p = \frac{I_{pyr}}{A\,dT/dt} = \frac{\Delta U_{pyr}}{AK_I \Delta T 2\pi f}, \qquad (1)$$

where A — the area of the electrodes (about 20 mm^2), ΔU_{pyr} and ΔT — pyroelectric signal amplitude and sample temperature change, respectively, and f — modulating frequency. In the case of step laser exposure, the sign and magnitude of the pyrocoefficient were calculated in accordance with (1) based on direct continuous measurements of the dynamics of the pyroelectric response changes $\Delta U_{pyr}(t)$ and the sample temperature $T(t)$ with subsequent calculation of its derivative.

Piezoelectric measurements were carried out using a Michelson –Morley single-beam interferometer [10,23–25], equipped with a lock-in amplifier SR830 (Stanford Research Systems Inc., Sunnyvale, CA, USA). A feedback system consisting of a piezoactuator P-841.01 and a piezocontroller E-709.SRG (Physik Instrumente, Karlsruhe, Germany) was used to stabilize the operating point and the length of the optical path. A heating table with a titanium layer as a heater, fixed between two copper plates of size 30 × 30 × 1.5 mm was used in measurements of the piezoelectric response at different temperatures. A system consisting of a temperature sensor Pt100 (Heraues Nexensos, Kleinostheim, Germany), software module MB110 (Owen, Moscow, Russia) and a programmable power supply ZUP60-3.5 (TDK-Lambda Corporation, Tokyo, Japan) was used to stabilize the temperature. The heating table was installed on a polytetrafluoroethylene base, thermally isolated from the rest of the system by polyurethane foam. The measurements were performed with exciting signal amplitude of 50–150 V and a frequency of 6–8 kHz, high enough to prevent any impact of extraneous mechanical resonances and electromagnetic noise. At least three measurements of the displacement amplitude were made, after which the results were averaged.

2. Results and discussion

All the studied crystals were rapidly heated to a temperature of about 70°C when the modulating laser radiation was turned on, after which an equilibrium with the environment was reached (Fig. 2, *a*). IR laser irradiation allows the sample to be heated to the required temperature, while the modulating laser is used for pyroelectric measurements. At the moment of the IR laser switching on, the sample temperature increases exponentially, which leads to a jump in the pyroelectric current (Fig. 2, *a*). The pyroelectric current I_{pyr} is proportional to the derivative of the sample temperature, consisting of the contribution of IR heating and the periodic contribution of the modulating laser. Upon reaching the operating temperature, I_{pyr} oscillates in phase with the intensity of the modulating laser, but with a phase shift by $\pi/2$ relative to the sample temperature, since it is proportional to the time derivative of temperature (Fig. 2, *b*). An abrupt increase of I_{pyr} is observed for the Gly-Thr crystal after switching on the IR laser (Fig. 2, *a*), which indicates a

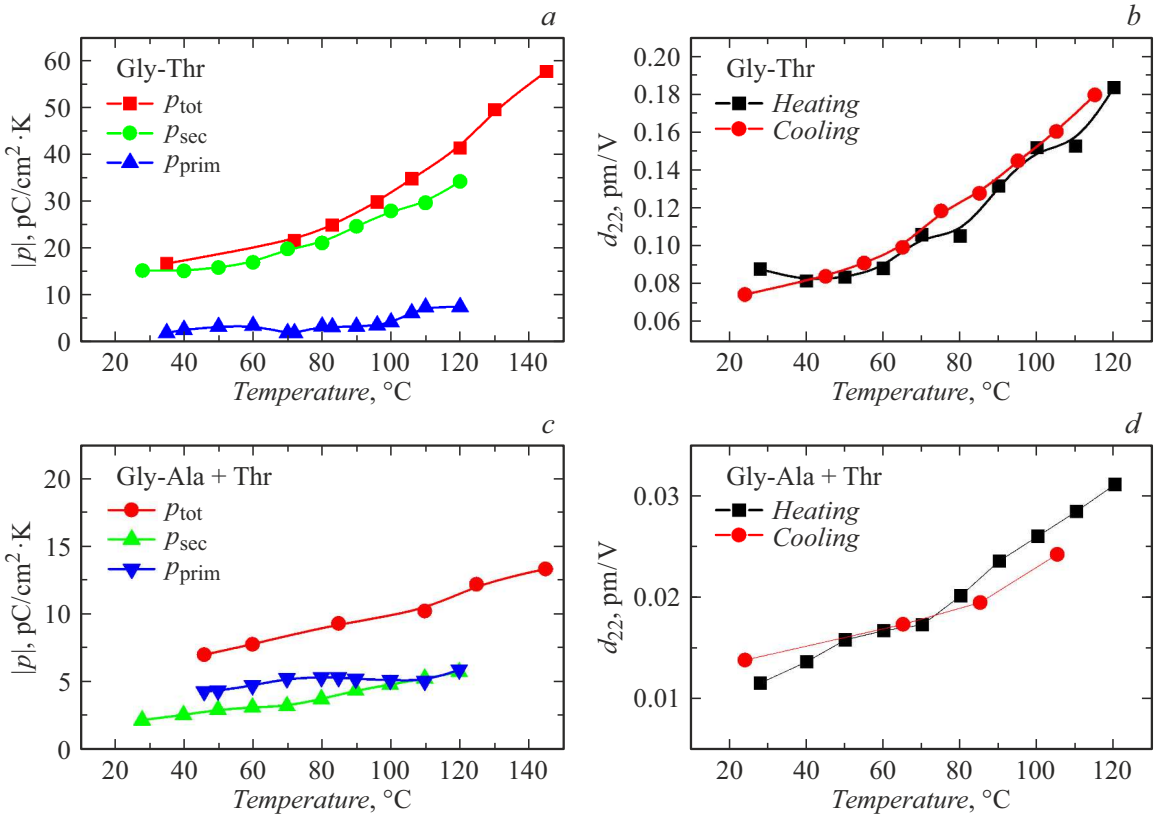

Figure 3. Temperature dependences of pyroelectric (a, c), p, and piezoelectric (b, d), d_{22}, coefficients in α-glycine crystals (a, b) Gly-Thr and (c, d) Gly-Ala+Thr.

positive sign of the pyroelectric coefficient but differs from the previously published data [14]. This difference may be related to the fact that the modulation technique used in the study [14] does not allow for a reliable determination of the sign of the coefficient, while the absolute values of the coefficients are consistent with each other.

A gradual relaxation of pyroelectric current I_{pyr} begins after its abrupt increase associated with the switching on the IR laser (Fig. 2, *a*). Approximation of this process using *erf*-function, as proposed in [10] (orange line (in online version) in Fig. 2, *a*), allowed determining the effective thickness of the pyroelectric layer δ, which was 1.6 and 0.86 cm for Gly-Thr and Gly-Ala+Thr crystals, respectively. These values are significantly larger than the actual thickness of the crystals (less than 500 μm), so it can be concluded that the measured pyroelectric response has a volumetric nature, and therefore includes both the contribution from polar doping molecules and from perturbations of the host crystal lattice [14].

The values of the pyroelectric coefficients p_{tot} obtained in the Gly-Thr crystal have a positive sign in the entire temperature range studied, whereas the absolute values of these coefficients are twice as large (Fig. 3, *a*) than previously reported [14]. This difference may be due to the different degree of doping of the samples. The crystals studied in [14] had a Thr concentration of about 5 wt.%, whereas crystals with a Thr concentration of about 0.5 wt.% were used in this work. Earlier, it was reported that the dielectric constant decreased with an increase in the dopant concentration in TGS crystals doped with Ala [26]. The nonlinear nature of the dielectric response was associated with the disordering of the dipole moments of glycine molecules and the dipole-dipole interaction between Gly and Ala molecules, depending on the doping level [26]. A similar mechanism takes place in the case of the polar properties of doped α-glycine crystals [14].

The values p_{tot} obtained in Gly-Ala+Thr crystals are also positive over the entire temperature range, but they are two times less than in Gly-Thr, and are less dependent on temperature (Fig. 3, *c*).

It was previously shown [14,20] that small Ala molecules cause a weak deformation of the glycine crystal lattice around the Ala molecule, and therefore the pyroelectric effect in such crystals is mainly originated by the dopants dipole moments. At the same time, larger Thr molecules lead to significant asymmetric displacements of the surrounding glycine molecules, and also contain an additional polar OH group. Therefore, the pyroelectric effect in such crystals will consist of contributions of both dopants dipole moments and dipole moments formed by local symmetry breaking of the host crystal lattice of glycine. We calculated the pyroelectric coefficients associated with the

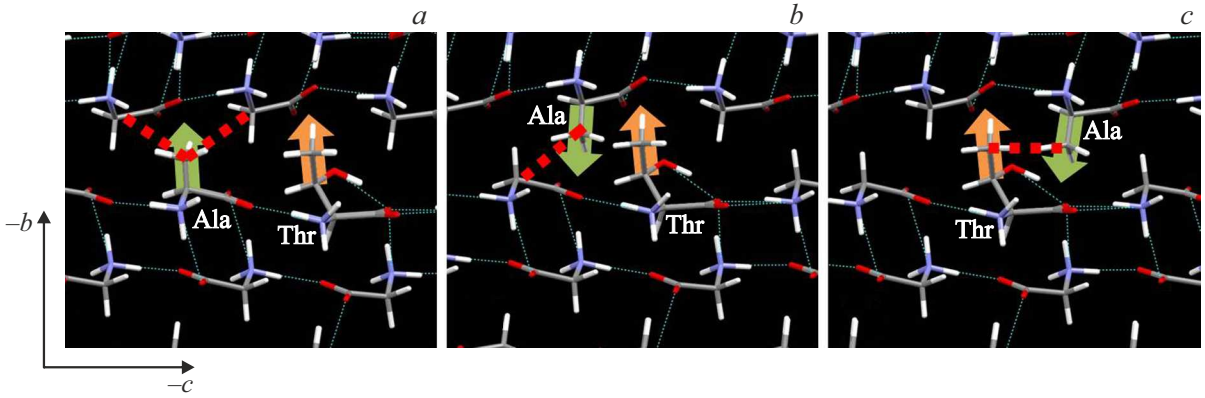

Figure 4. Three possible configurations of the dopant complex Ala-Thr in the lattice of α-glycine. Green and orange arrows (in online version) indicate the directions of the dipole moments of the side branches; thick red dotted lines (in online version) show the directions of the greatest repulsive interaction between molecules.

primary and secondary pyroelectric effects to quantify these contributions.

The contribution of the secondary effect can be estimated based on measurements of the piezoelectric response of the crystals. Nonlinear temperature dependences of the piezoelectric coefficient d_{22} for Gly-Thr and Gly-Ala+Thr crystals are shown in Fig. 3, *b, d*. Both crystals show a weak but noticeable piezoelectric response, with d_{22} coefficient in the Gly-Ala+Thr crystal (0.01−0.03 pm/V) in 2−3 times less than in the Gly-Thr crystal (0.06−0.2 pm/V). This difference is similar to that observed for pyroelectric coefficients. No hysteresis was observed in the heating-cooling cycles (Fig. 3, *b, d*).

Secondary pyroelectric coefficient $p_{sec} = d_{22}\gamma_2 Y_2$, where $\gamma_2 = 7 \cdot 10^{-5}\,\mathrm{K}^{-1}$ — coefficient of thermal expansion (determined from data in [27]) and $Y_2 = 26\,\mathrm{GPa}$ — Young's modulus in the (010) direction [28]. The obtained temperature dependences of p_{sec} for both crystals are shown in Fig. 3, *a, c*. The difference between the total and secondary pyroelectric coefficients shows the contribution of the primary pyroelectric coefficient, p_{prim}, arising due to the spontaneous polarization and, consequently, the orientation of the dipole moments of doping molecules. The values of p_{prim} are small for Gly-Thr crystal, whereas the contribution of p_{sec} to the total pyroelectric coefficient p_{tot} reaches 80−90%. Such ratio of contributions differs from what was observed earlier in α-glycine crystals with modified surface layers, where the contribution of the secondary pyroelectric effect was less than 14% [10]. The higher contribution of the coefficient p_{sec} also does not coincide with the assumption expressed in [14] that Thr molecules have the same contributions to primary and secondary pyroelectric effects. Apparently, the contribution of the distorted crystal lattice exceeds the contribution from the dopants dipole moments for crystals with a high level of doping.

At the same time, in Gly-Ala+Thr crystals, the values of p_{sec} are noticeably smaller than in Gly-Thr crystals, and are close to p_{prim}, which indicates the non-additive effect of double doping on the distortion of the crystal lattice, the effect of which becomes comparable with the contribution of the dopants dipole moments. The mechanism of such influence has yet to be studied.

A quantitative assessment of the effect of doping on the crystal lattice was done by the determination of the interaction energies between molecules in the crystal lattice of pure α-glycine and in doped lattices, where some glycine molecules are replaced by Ala and Thr. Calculations were made using the empirical pair potential UNI [29–31] in CCDC Mercury 2022 2.0 [32]. The typical interaction energies between neighboring Gly molecules in an ideal crystal lattice of α-glycine range from −6 to −14 kJ/mol. The strongest interaction with an energy of about −40 kJ/mol is observed between mirror-inverted molecules forming a bilayer. The negative sign of energy corresponds to the attraction between glycine molecules, which stabilizes the crystal lattice.

When analyzing the effect of double doping on the crystal lattice, two situations need to be considered: (1) low doping and (2) strong doping. In the case of a low doping, Ala and Thr molecules occupy lattice sites located far from each other and do not interact with each other, whereas in the case of strong doping, a high concentration of dopants inevitably leads to the approaching of Ala and Thr molecules and the formation of dopant complexes with different relative orientations of the side branches of the molecules. However, a noticeable dipole-dipole interaction between dopants can lead to the formation of similar complexes in solution, which are subsequently embedded in the glycine crystal either in its original form or in a modified form.

It is known that the interactions of the side branches of doping amino acids have a significant effect on the induced polarization [14]. Three different dopant complexes can be considered (Fig. 4): (1) Ala and Thr molecules are in the same crystallographic layer, and their dipole moments are co-directed (Fig. 4, *a*); (2) Ala and Thr molecules are located at lattice sites in neighboring crystallographic layers, and their dipole moments are directed in opposite directions (Fig. 4, *b*); (3) the configuration is similar to (2), but the

OH group of the Thr molecule additionally interacts with the CH_3 group of the Ala molecule (Fig. 4, *c*).

In the first case (Fig. 4, *a*), the interaction between Ala and Gly molecules reaches 80 kJ/mol (red dotted lines (in online version)), which indicates that in such a configuration, Ala molecules cause strong mechanical stresses in the glycine crystal lattice. At the same time, the interaction energy between Ala and Thr molecules is relatively small, about −23 kJ/mol, which probably allows to stabilize the complex. The interaction energy between Ala and Thr molecules in the second dopant complex is 9.5 kJ/mol at the interaction of Ala-Gly to 47 kJ/mol (Fig. 4, *b*). This configuration is apparently less stable than the first one. In the third dopant complex (Fig. 4, *c*), the energy of the repulsive interaction between Ala and Thr molecules reaches 146 kJ/mol, which also indicates the instability of the complex.

Thus, the first configuration of the dopant complex is the most stable in glycine crystals with double doping. Since, as shown above, the secondary pyroelectric coefficient is noticeably less in crystals with double doping than in Gly-Thr crystals, the non-additive effect of the double doping on the crystal lattice distortion may be attributable to the presence of a strong interaction between dopant molecules in such configuration. The second and third types of dopant complexes are also possible in real crystals. However, the mechanisms of their stabilization have yet to be clarified.

Conclusion

Pyroelectric and piezoelectric properties of centrosymmetric crystals of α-glycine doped with threonine molecules and crystals with double doping with threonine and alanine were investigated in this work. The separation of primary and secondary pyroelectric effects showed that in crystals with single doping, pyroelectric properties are mainly associated with the distortions of the crystal lattice, whereas for crystals with double doping, a balance between the lattice distortions and the interaction of dopants is observed. Analysis of the interaction energy between dopants and the crystal lattice allowed us to determine the most stable configuration of the dopant complex in crystals with double doping. This configuration is consistent with the observed lower value of the secondary pyroelectric coefficient, compared with Gly-Thr crystals, however, the mechanism of the non-additive effect on the distortion of the crystal lattice has yet to be clarified. The results obtained expand the understanding of the nature of the polar properties occurrence in doped centrosymmetric molecular crystals.

Acknowledgments

The authors thank S. Dishon and I. Lubomirsky for the crystals provided for the study.

Funding

This study was funded by RFBR and MOST (grant № 19-52-06004), as well as by the Ministry of Science and Higher Education of the Russian Federation (state assignment FEUZ-2023-0017 and 0040-2019-0019). The equipment of the Ural Center for Shared Use „Modern Nanotechnology“ of the Ural Federal University (reg. number 2968), supported by the Ministry of Science and Higher Education of the Russian Federation (project № 075-15-2021-677), was used.

Conflict of interest

The authors declare that they have no conflict of interest.

References

[1] J.F. Nye. *Physical Properties of Crystals* (Clarendon Press, 1957)
[2] S.B. Lang. Phys. Today, **58** (8), 31 (2005). DOI: 10.1063/1.2062916
[3] I. Lubomirsky, O. Stafsudd. Rev. Sci. Instrum., **83**, 051101 (2012). DOI: 10.1063/1.4709621
[4] A. Thakre, A. Kumar, H.-C. Song, D.-Y. Jeong, J. Ryu. Sensors, **19**, 2170 (2019). DOI: 10.3390/s19092170
[5] S. Korkmaz, I.A. Kariper. Nano Energy, **84**, 105888 (2021). DOI: 10.1016/j.nanoen.2021.105888
[6] H. Ryu, S.-W. Kim. Small, **17**, 1903469 (2021). DOI: 10.1002/smll.201903469
[7] H. He, X. Lu, E. Hanc, C. Chen, H. Zhang, L. Lu. J. Mater. Chem. C, **8**, 1494 (2020). DOI: 10.1039/c9tc05222d
[8] A.S. Bhalla, R.E. Newnham. Phys. Status Solidi A, **58**, K19−K24 (1980). DOI: 10.1002/pssa.2210580146
[9] W. Xusheng. Ferroelectr. Lett. Sect., **12**, 115 (1991). DOI: 10.1080/07315179108201147
[10] S. Dishon, A. Ushakov, A. Nuraeva, D. Ehre, M. Lahav, V. Shur, A. Kholkin, I. Lubomirsky. Materials, **13**, 4663 (2020). DOI: 10.3390/ma13204663
[11] K.L. Acosta, S. Srivastava, W.K. Wilkie, D.J. Inman. Compos. B Eng., **177**, 107275 (2019). DOI: 10.1016/j.compositesb.2019.107275
[12] C.-P. Ye, T. Tamagawa, D.L. Polla. J. Appl. Phys., **70**, 5538 (1991). DOI: 10.1063/1.350212
[13] G. Velarde, S. Pandya, L. Zhang, D. Garcia, E. Lupi, R. Gao, J.D. Wilbur, C. Dames, L.W. Martin. ACS Appl. Mater. Interf., **11**, 35146 (2019). DOI: 10.1021/acsami.9b12191
[14] E. Meirzadeh, I. Azuri, Y. Qi, D. Ehre, A.M. Rappe, M. Lahav, L. Kronik, I. Lubomirsky. Nature Commun., **7**, 13351 (2016). DOI: 10.1038/ncomms13351
[15] H.V. Alexandru. Ann. NY. Acad. Sci., **1161**, 387 (2009). DOI: 10.1111/j.1749-6632.2008.04080.x
[16] R.B. Lal, A.K. Batra. Ferroelectrics, **142**, 51 (1993). DOI: 10.1080/00150199308237884
[17] H.V. Alexandru, C. Berbecaru, F. Stanculescu, L. Pintilie, I. Matei, M. Lisca. Sens. Actuat. A, **113**, 387 (2004). DOI: 10.1016/j.sna.2004.03.046
[18] M. Lusi. Cryst. Eng. Commun., **20**, 7042 (2018). DOI: 10.1039/C8CE00691A

[19] Z. Qin, C. Gao, W.W.H. Wong, M.K. Riede, T. Wang, H. Dong, Y. Zhena, W. Hu. J. Mater. Chem. C, **8**, 14996 (2020). DOI: 10.1039/D0TC02746D
[20] M.S. Cedric. *Physical properties of crystals of the triglycine sulfate family* (Science and Technology, Minsk, 1986)
[21] V.Yu. Torbeev, E. Shavit, I. Weissbuch, L. Leiserowitz, M. Lahav. Cryst. Growth Des., **5**, 2190 (2005). DOI: 10.1021/cg050200s
[22] G.Yu. Sotnikova, G.A. Gavrilov, A.A. Kapralov, K.L. Muratikov, E.P. Smirnova. Rev. Sci. Instrum., **91**, 015119 (2020). DOI: 10.1063/1.5108639
[23] E. Mishuk, A. Ushakov, E. Makagon, S.R. Cohen, E. Wachtel, T. Paul, Y. Tsur, V.Y. Shur, A. Kholkin, I. Lubomirsky. Adv. Mater. Interf., **6**, 1801592 (2019). DOI: 10.1002/admi.201801592
[24] E. Mishuk, A.D. Ushakov, S.R. Cohen, V.Y. Shur, A.L. Kholkin, I. Lubomirsky. Sol. State Ion., **327**, 47 (2018). DOI: 10.1016/j.ssi.2018.10.012
[25] A.D. Ushakov, N. Yavo, E. Mishuk, I. Lubomirsky, V.Y. Shur, A.L. Kholkin. KnE Mater. Sci., **2016**, 177 (2016). DOI: 10.18502/kms.v1i1.582
[26] P.K. Bajpai, A.L. Verma. Spectrochim. Acta A, **96**, 906 (2012). DOI: 10.1016/j.saa.2012.06.007
[27] P. Langan, S.A. Mason, D. Mylesc, B.P. Schoenborn. Acta Cryst. B, **58**, 728 (2002). DOI: 10.1107/S0108768102004263
[28] I. Azuri, E. Meirzadeh, D. Ehre, S.R. Cohen, A.M. Rappe, M. Lahav, I. Lubomirsky, L. Kronik. Angew. Chem. Int. Ed., **54**, 13566 (2015). DOI: 10.1002/anie.201505813
[29] A. Gavezzotti. Acc. Chem. Res., **27**, 309 (1994). DOI: 10.1021/ar00046a004
[30] A. Gavezzotti, G. Filippini. J. Phys. Chem., **98**, 4831 (1994). DOI: 10.1021/j100069a010
[31] A. Gavezzotti. Crystallogr. Rev., **7**, 5 (1998). DOI: 10.1080/08893119808035402
[32] P.R. Edgington, P. Mc Cabe, C.F. Macrae, E. Pidcock, G.P. Shields, R. Taylor, M. Towler, J. van de Streek. J. Appl. Crystallogr., **39**, 453 (2006). DOI: 10.1107/S002188980600731X

Translated by A.Akhtyamov